

# We are IntechOpen, the world's leading publisher of Open Access books Built by scientists, for scientists

6,900

Open access books available

186,000

International authors and editors

200M

Downloads

Our authors are among the

154

Countries delivered to

TOP 1%

most cited scientists

12.2%

Contributors from top 500 universities



WEB OF SCIENCE™

Selection of our books indexed in the Book Citation Index  
in Web of Science™ Core Collection (BKCI)

Interested in publishing with us?  
Contact [book.department@intechopen.com](mailto:book.department@intechopen.com)

Numbers displayed above are based on latest data collected.  
For more information visit [www.intechopen.com](http://www.intechopen.com)



---

# Nanopowders Production and Micron-Sized Powders Spheroidization in DC Plasma Reactors

---

Andrey Samokhin, Nikolay Alekseev,  
Mikhail Sinayskiy, Aleksey Astashov,  
Dmitrii Kirpichev, Andrey Fadeev, Yurii Tsvetkov and  
Andrei Kolesnikov

Additional information is available at the end of the chapter

<http://dx.doi.org/10.5772/intechopen.76262>

---

## Abstract

Technology for metal and inorganic compounds nanopowders production in DC arc plasma reactors has been developed. Similar DC arc plasma reactors were used for micron-sized powders spheroidization. Results of experimental studies are presented. Formation of nanoparticles via different mechanisms as well as mass transfer of nanopowders to the reactor cooling surfaces are discussed. Heat flux distribution along the reactor wall and its influence on the evolution of nanoparticles in the deposited layer are investigated. Effects of plasma torch and confined jet reactor operation parameters on the granulometric, phase and chemical composition of nanopowders are discussed. Potential of the confined plasma jet apparatus for micron-sized metal and composite particles spheroidization is demonstrated.

**Keywords:** thermal plasma, DC arc plasma torch, nanopowder, synthesis, reactor, spheroidization, metals, inorganic compounds

---

## 1. Introduction

Nanosized powders of elements and their inorganic compounds are the basis for development of various nanostructured materials. These materials include nanostructured functional ceramics, hard alloys with increased wear resistance and toughness, dispersion hardened and modified structural alloys with enhanced performance characteristics, nanostructured protective

thermo-, corrosion and wear-resistant coatings, polymer composites with fillers and inorganic nanoparticle modifiers for alloys [1–9].

Various techniques are used for nanopowders synthesis, including processing in gas, liquid and solid phases. Such methods employ physical and chemical deposition from gas phase, precipitation from solutions, mechanical grinding, etc. The formation of nanoparticles by homogeneous nucleation in supersaturated vapors followed by nanoparticles growth via condensation and coagulation is the basis of any gas phase nanoparticles manufacturing process. Fast cooling of saturated vapors or gas phase chemical reactions produce supersaturated vapors. Depending on the method used, processes for nanopowders manufacturing in gas phase include flame synthesis, evaporation in high-energy beams (laser radiation, accelerated electrons, focused microwave radiation), and plasmachemical synthesis in DC arc plasma.

Plasmachemical synthesis is the most versatile method for manufacturing of metal and inorganic compounds nanopowders, or nanopowders mixtures using inert, reducing and oxidizing atmospheres with controlled composition. Main advantages of nanopowders plasmachemical synthesis are:

1. Various types of nanopowders (individual elements, compounds and mixtures) can be produced;
2. Physical and chemical characteristics of the nanopowders can be controlled and nanopowders with required parameters (purity, chemical and phase compositions, specific surface) can be produced;
3. Plasma reactors have small dimensions and high production rate;
4. Traditional commonly applied raw materials can be used;
5. Process can be easily scaled-up from laboratory setup to the level of industrial equipment with high productivity.

High efficiency and other technological characteristics of nanopowder production in plasma testify to the competitiveness of the plasma method and wide possibilities for its application. As estimates show, the cost of nanopowders produced using plasma technologies at mass production level should slightly differ from the cost of “traditional” powders of this nomenclature. Plasma technologies can be considered as an effective way of obtaining a wide range of nanopowders. Thermal plasma can be generated using various types of electric discharges [10]. They include DC arc discharge, high-frequency (radio frequency) induction plasma discharge (RF), microwave plasma (UHF), as well as combined discharges.

At present, RF plasma reactors developed and manufactured by TEKNA [11] are widely used for nanopowders production. When operating electrodeless RF and microwave plasmatrons, the impurities (such as electrode’s erosion products) in the nanopowders are absent, but it might appear when using DC arc plasma generators. However, it should be borne in mind that the present value of 1 kW of power generated by RF and microwave plasma torches is up to 3 times higher than the cost of plasma generation in DC arc plasma torches [12]. Besides,

the power of modern DC arc plasma torches reaches 3–5 MW with a service life of up to 103 h [13, 14], while the power of existing RF plasmotrons does not exceed 1 MW. The usage of V-shaped DC arc plasmotrons where tungsten electrodes operate in an argon inert gas medium [15] allows to minimize the presence of impurities of the electrode material in the thermal plasma flow and to ensure the production of high-purity target products. Westinghouse Plasma Corporation developed plasmotrons with a power of 300–2400 kW and thermal efficiency of 70–85%. Such devices are used in waste materials processing and metallurgical furnaces operations [14]. DC plasma torches have high energy efficiency and can be used in the realization of high-temperature processes on an industrial scale. This paper provides a review of the research in the field of nanopowders synthesis and processing (spheroidization) of micron sized powders in thermal plasma flows generated by DC arc plasma torches. The research was carried out at the Institute of Metallurgy and Materials Science (IMET RAS) in collaboration with partners over recent years.

## 2. Plasmachemical reactor

IMET RAS developed DC arc plasma torches with a nominal power of 30–150 kW with self-setting arc length and gas discharge stabilization, as well as plasmotrons with an inter-electrode insert. The torches were used for the generation of thermal plasma in IMET laboratories and pilot plants. The plasma torches operated with reducing, oxidizing and inert gases and their mixtures and provided stable generation of plasma jets with an equilibrium temperature of up to 4000–8000 K (for molecular gases) and up to 12,000 K (for monatomic gases). The torches were used for both nanopowder production processes and for spheroidization processes. Plasma synthesis of nanopowders includes a complex set of physicochemical processes occurring in turbulent gas-dispersed non-isothermal flows. At present, plasma reactors with confined jet are widely used for nanopowders production. In confined jet reactor, the plasma jet flows into the volume of the reactor, which is confined by the cooled cylindrical surface. The ratio of the torch nozzle diameter to the reactor's diameter is of the order of 10. The plasma jet can be generated by any type of plasma generator (DC arc discharge, high frequency discharge, microwave discharge). When a plasma jet outflows from plasma torch into reactor's volume, a rapid temperature drop occurs, resulting in supersaturated vapors formation. Vapors condensation leads to the nanoscale particles formation. Evolution of nanoparticles granulometric composition occurs in the reactor's volume because of their condensation and coagulation growth. Phase and chemical compositions of nanoparticles can also change. Control of nanoparticles formation is achieved by variation of such operational parameters as plasma jet chemical composition, enthalpy and flow rate; concentrations of reagents in the reactor; and parameters of the reagents injection into the plasma jet. If solid powder is used as raw material, the initial size of the solid particles has significant effect of nanoparticles formation.

During nanoparticles formation in the volume of plasma reactor, they move toward internal cooled surfaces of the reactor. The layer of nanoparticles is formed at these surfaces. The deposited layer evolution is affected by heat flux from the high temperature gas flow inside

the reactor. The evolution of nanoparticles in the layer is determined by the temperature distribution and lifetime of the layer, and the temperature distribution depends in turn on the temperature of the cooled surface, the density of the mass flux of the deposited nanoparticles, and the density of the heat flux passing through the layer. Under plasmachemical synthesis conditions the layer thickness, as well as its thermal resistance, are increased in time. The unsteady temperature field in the layer can lead to the time changes of the layer's structure, phase and chemical composition. These changes are due to chemical reactions, phase transformations, and particles sintering. All these changes occur when the temperature in the growing layer increases. To obtain the nanopowder with required specifications, where nanoparticles retain the properties determined by the conditions of their formation in the gas stream, it is necessary to exclude or minimize the possibility of physicochemical transformations in the layer of precipitated particles. It is necessary to prevent the layer's temperature rise above certain threshold values. These values are the temperatures of nanoparticles characteristic chemical and phase transformations, and temperatures related to nanoparticles growth due to their contacts in the layer. Nanoparticles are formed in the plasma process inside the reaction zone, but possible nanoparticles transformations in the growing layer on the reactor's surfaces might change the properties of nanoparticles and become a problem. This problem is important for the realization of controlled plasma synthesis of nanopowders with given properties.

An unlimited growth of the nanoparticles layer thickness will inevitably lead to an increase in the layer's temperature resulting in the particles sintering and coarsening, as well as possible change in their phase and chemical composition. These effects will be most pronounced for nanoparticles with a low temperature of possible physicochemical transformations, especially for particles with low melting point. Thus, to obtain the nanopowder with required specifications, the nanoparticles physical and chemical transformations in the deposited layer have to be blocked. To achieve this, the thickness of this layer, formed on the stationary cooled reactor's surface, must be limited to a certain value. For particular target nanopowders, the size of the precipitating nanoparticles, the initial temperature of the deposition surface and the heat flux density from the high temperature stream to the deposition surface will determine this limiting layer's thickness.

### **3. Heat transfer to the wall of reactor**

The investigations of metal and inorganic compounds nanopowders synthesis included experimental studies of heat and mass transfer in a confined plasma jet reactor [16].

Following topics were studied:

1. heat flux density distribution along the reactor's length to the nanoparticle deposition surface
2. mass flux density distribution of deposited nanoparticles along the reactor's length

3. physical and chemical properties of nanopowders deposited on the surface in various zones under various process parameters

A cylindrical sectioned plasma reactor with confined jet stream was used. Reactor had diameter and length of 200 and 600 mm correspondently (**Figure 1**) [17]. The length of the sections varied in the range 70–130 mm. DC arc plasma torch with a rated power of 25 kW was used for thermal plasma generation. Nitrogen, hydrogen-nitrogen mixture (22 vol. % H<sub>2</sub>), and air were used as plasma-forming gases. The synthesized nanoparticles were deposited on the reactor's walls and partially removed with the exhaust gases into the filtration apparatus.

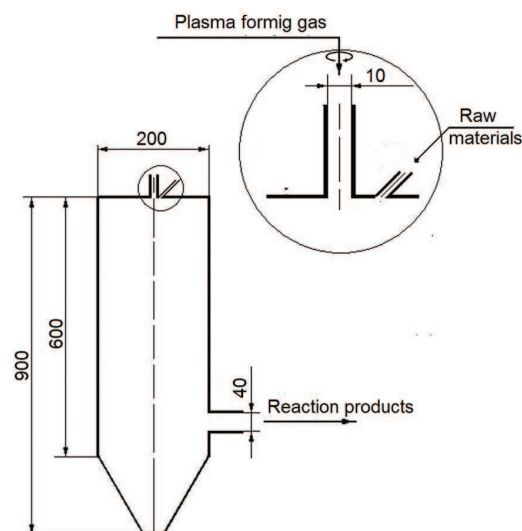


**Figure 1.** General view of 30 kW plasma setup.

Following processes were carried out in the reactor:

- Copper nanopowders production via evaporation-condensation of dispersed copper (raw particles less than 40  $\mu\text{m}$ ) in a nitrogen plasma;
- Production of tungsten nanopowders by reduction of dispersed tungsten trioxide  $\text{WO}_3$  (raw particles less than 40  $\mu\text{m}$ ) in hydrogen-nitrogen plasma
- Production of aluminum oxide nanopowders by oxidation of disperse aluminum (ASD-4, raw particles less than 10  $\mu\text{m}$ ) in air plasma;
- Production of multicomponent composition in tungsten-carbon system (W-C) via interaction of dispersed tungsten trioxide  $\text{WO}_3$  (raw particles less than 40  $\mu\text{m}$ ) with methane in hydrogen-nitrogen plasma.

The reactions underlying these processes differ in thermal effects calculated under standard conditions. Copper evaporation-condensation reaction has a zero thermal effect, the reaction of tungsten trioxide reduction by hydrogen is weakly endogenous (0.5 MJ/kg  $\text{WO}_3$ ), and the oxidation of aluminum by oxygen has a strong exogenous character (31 MJ/kg Al).

The experiments were carried out in the following parameters variation range:

Plasma forming gas flow rate	0.85–2 st. $\text{m}^3/\text{hour}$ ,
Plasma torch nozzle diameter	6–12 mm,
Plasma flow enthalpy at the reactor inlet	13–29 MJ/st. $\text{m}^3$ ,
Plasma flow power	6.6–12.3 kW,
Flow rate of dispersive raw material	1.0–7.0 g/min,
Duration of experiments	5–80 min

It was experimentally observed that when clean (no nanoparticles are present) nitrogen plasma jet enters the reactor, the heat flux density distribution along the reactor's length shows maximum in the attachment region of the high-temperature flow to the reactor wall, which is typical for the separated flows in the channels with sudden expansion. The value of the heat flux density is determined mainly by the plasma flow power at the reactor's inlet and in our experiments it varied in the range 25–45  $\text{kW}/\text{m}^2$ . The maximum value of the heat flux density exceeds by 2.5–3 times the values at initial and final sections of the reactor. Distribution of normalized heat flux density, i.e. flux related to the magnitude of the maximum, remains practically unchanged in the whole experimental range of input parameters variation (thermal power, flow rate and enthalpy) (**Figure 2A**). The presence of hydrogen in nitrogen practically did not change the heat fluxes values in the reactor. A decrease of the torch nozzle diameter from 10 mm to 6 mm led to the relocation of flow attachment region further downstream from the reactor inlet, and location of maximum wall heat flux changed accordingly.

In experiments when nanopowders of copper, tungsten, and W-C composition were synthesized, it was found that heat flux density distribution along the reactor length also had extremum (**Figure 2B**), as in the case of the flow containing no dispersed particles. But for a two-phase

flow (gas + particles) some increase in the heat flux density at the reactor initial sections was observed. This may be due to the radiation from condensed particles to the wall in the highest temperature zone of the reactor. This zone is located at the initial section of the plasma jet.

When aluminum oxide nanopowder was synthesized by oxidation of aluminum powder in air plasma jet, the significant differences in heat fluxes distribution in comparison with other realized processes were observed (**Figure 3**). With an increase in raw aluminum powder feed

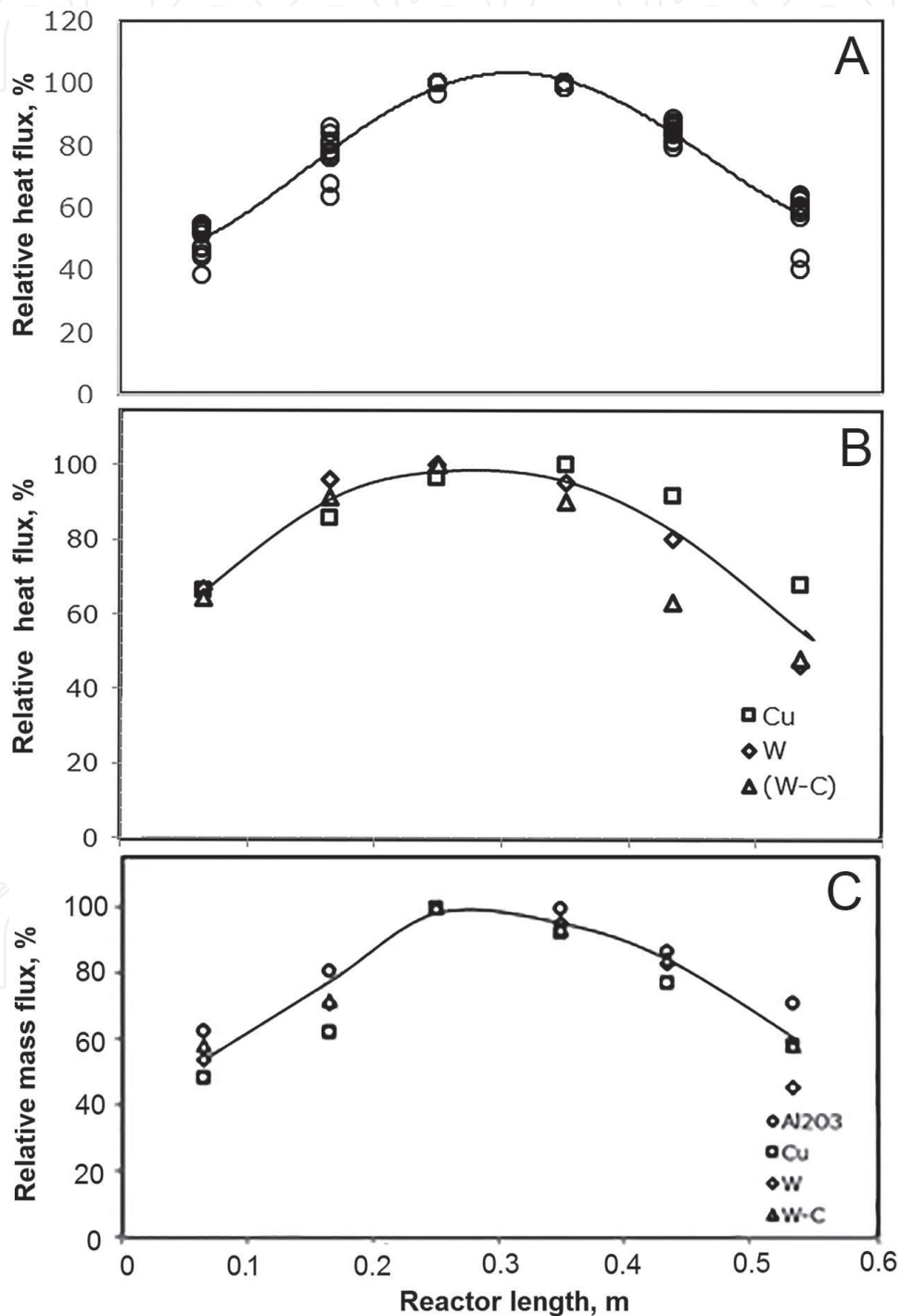


Figure 2. Normalized heat flux and mass flux distributions at plasma reactor wall.

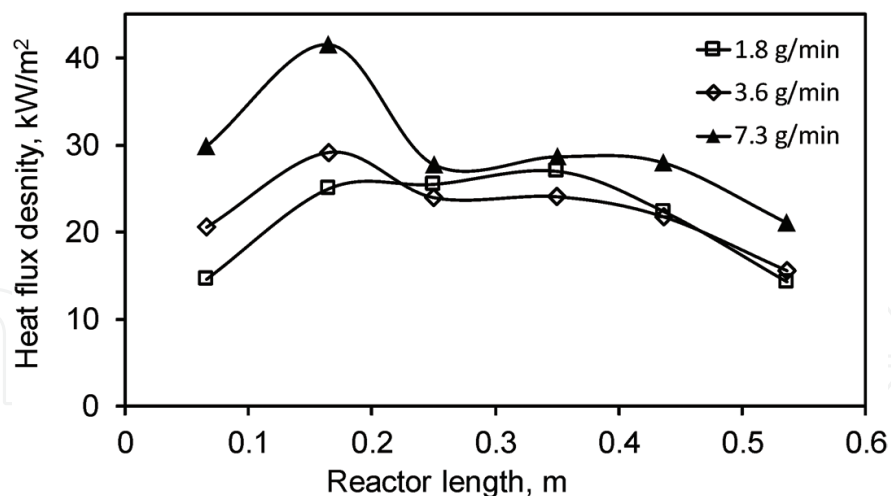


Figure 3. Heat flux density distribution in  $\text{Al}_2\text{O}_3$  nanopowder synthesis for various Al feed rates.

rate, the maximum heat flux density shifts toward the beginning of the reactor, while its magnitude increases due to additional heat release as a result of the highly exogenous reaction of aluminum oxidation by air oxygen. Depending on the raw material feed rate, the additional power released as a result of this reaction was equal to 10–40% of the plasma jet power. The local heat flux density on the reactor wall in the studied nanopowder syntheses varied in the range 10–40  $\text{kW/m}^2$ . It follows from experiments that non-uniform wall heat flux density distribution exists in plasma reactor with a confined jet flow, and the exogenous reactions with a pronounced thermal effect can exert a significant influence on the wall heat flux distribution. Some nanoparticles degradation might occur inside the deposited nanoparticles layer in the area of maximal heat flux.

#### 4. Mass transfer to the wall of reactor and formation of particle's layer

In the near-wall region of the plasma reactor, the nanoparticles transfer occurs under conditions when the average size of the nanoparticles is smaller or commensurable with the mean free path of the gas molecules, so the deposition of nanoparticles onto reactor wall from turbulent non-isothermal flow will be determined by the resulting effect of thermophoresis and Brownian diffusion [18]. The performed experiments have demonstrated that the deposited particles distribution along the reactor length has single extremum (Figure 2C), while the location of the maximum particle mass flux density coincides with the location of the maximum heat flux density. A similar particle flux density distribution is observed for all the studied processes, including aluminum oxide synthesis, where heat flux density distribution could have a bimodal character. The mass flow density is determined by the condensed phase mass concentration in the solid–gas flow, with the maximum value of the mass flow density exceeding by up to 2–3 times the mass flow density at the initial and final sections of the reactor.

For all the processes in the studied parameter variation ranges a high degree of nanoparticles deposition on the reactor surface is observed. The deposited mass is equal to 40–80% of the total

mass of synthesized nanopowder. Consequently, the final properties of the produced nanopowders are largely determined by the properties of the product that is precipitated exactly in the reactor. The degree of nanoparticles deposition decreases with increasing of the process duration (thickness of the deposited layer of nanoparticles) and with an increase in the raw materials feed rate (processing rate). It follows from analysis of experimentally found heat flux density distributions and mass fluxes density distributions along the reactor wall that the maximum heat flux position coincides with location of maximum mass flux, where growth of the nanoparticle layer occurs at the maximum rate. The effect of heat flux makes possible nanoparticles transformations such as sintering, chemical interaction with the active gaseous medium, and phase transformations most probable exactly in this region of the reactor internal surface.

The layers of deposited nanoparticles had an extremely low bulk density, equal to 3–8% of the theoretical density. The deposited layers thickness varied from 0.05 to 2.7 mm in the experiments. Sintering of deposited nanoparticles near the maximum heat flux density location was noted only for copper nanopowder, where the melting point of the metal is 1360 K. A slight change in the average nanoparticle size inside the deposited layer along the reactor length is noted for other nanopowders (W, Al<sub>2</sub>O<sub>3</sub>, (W-C)), whose materials have much higher melting point. General list of nanopowder syntheses, performed in confined jet reactor, is given in **Table 1**. Some syntheses (AlN, AlON) were carried out in a combined reactor with disperse raw materials pre-evaporation in a heat-insulated channel followed by gas chemical quenching.

No	Nanopowder	Initial reagents	Plasma forming gas	Properties of nanopowders		
				Phase composition	Specific surface area, m <sup>2</sup> /g	Impurities
Metals						
1	W, Mo, Ni, Co, Re	Me <sub>x</sub> O <sub>y</sub> , H <sub>2</sub> , C <sub>3</sub> H <sub>8</sub> + air	H <sub>2</sub> + N <sub>2</sub> , C <sub>3</sub> H <sub>8</sub> + air	Me	2–30	[O]
2	Cu	CuCl	H <sub>2</sub> + N <sub>2</sub>	Cu, Cu <sub>2</sub> O, CuO, CuCl	2–5	[Cl], [O]
		Cu(HCOO) <sub>2</sub>	N <sub>2</sub>	Cu, Cu <sub>2</sub> O, CuO	2–7	[C]
		Cu(CH <sub>3</sub> COO) <sub>2</sub> · H <sub>2</sub> O	N <sub>2</sub>	Cu, Cu <sub>2</sub> O, CuO	5–35	[C]
		Cu(re-condensation)	N <sub>2</sub>	Cu, Cu <sub>2</sub> O, CuO	20–36	[O]
Metal composites						
3	W-Ni-Fe (W – 95 mass %)	WO <sub>3</sub> , NiO, Fe <sub>2</sub> O <sub>3</sub> , H <sub>2</sub>	H <sub>2</sub> + N <sub>2</sub>	W, Ni-Fe	5–12	[O]
4	W-Cu (W - 80 mass %)	WO <sub>3</sub> , CuO	H <sub>2</sub> + N <sub>2</sub>	W, Cu	4–8	[O]
5	Ag-SnO <sub>2</sub>	Ag, SnO <sub>2</sub>	air	Ag, SnO <sub>2</sub>	4–25	
Nitride, carbides, carbonitrides						
6	TiN	Ti, (TiH <sub>2</sub> ), N <sub>2</sub>	N <sub>2</sub>	TiN	10–20	[Ti] <sub>metal</sub>
		TiCl <sub>4</sub> , H <sub>2</sub> , N <sub>2</sub>	H <sub>2</sub> + N <sub>2</sub>	TiN	11–39	[Cl]

No	Nanopowder	Initial reagents	Plasma forming gas	Properties of nanopowders		
				Phase composition	Specific surface area, m <sup>2</sup> /g	Impurities
7	AlN	Al, NH <sub>3</sub> , N <sub>2</sub>	N <sub>2</sub>	AlN	75–100	[Al] <sub>metal</sub>
8	TiC	TiCl <sub>4</sub> , H <sub>2</sub> , CH <sub>4</sub>	H <sub>2</sub> + Ar	TiC	15–45	[Cl]
9	TiCN	TiCl <sub>4</sub> , H <sub>2</sub> , N <sub>2</sub> , CH <sub>4</sub>	H <sub>2</sub> + N <sub>2</sub>	TiN	13–23	[Cl]
10	SiC	SiCl <sub>4</sub> , H <sub>2</sub> , CH <sub>4</sub>	H <sub>2</sub> + Ar	B - SiC	20–75	[Cl]
11	W - C (C <sub>total</sub> = 6.2 mass %)	WO <sub>3</sub> , CH <sub>4</sub> , H <sub>2</sub>	H <sub>2</sub> + N <sub>2</sub>	WC <sub>1-x</sub> , W <sub>2</sub> C, W, C	15–25	
Oxides						
12	Al <sub>2</sub> O <sub>3</sub>	Al, O <sub>2</sub>	Air	δ - Al <sub>2</sub> O <sub>3</sub>	15–50	
13	Al <sub>2</sub> O <sub>3</sub> - MeO (Me = Mg, Co)	Al, Me, O <sub>2</sub>	Air	MeAl <sub>2</sub> O <sub>4</sub> (spinel)	12–16	
14	AlON	Al, NH <sub>3</sub> , N <sub>2</sub> , O <sub>2</sub>	N <sub>2</sub>	AlON	20–70	[Al] <sub>metal</sub>
15	TiO <sub>2</sub>	TiCl <sub>4</sub> , O <sub>2</sub>	O <sub>2</sub> + Ar	TiO <sub>2</sub> (rutile + anatase)	10–120	[Cl]
16	SiO <sub>2</sub>	SiCl <sub>4</sub> , O <sub>2</sub>	O <sub>2</sub> + Ar	amorphous	200–300	[Cl]
17	ZrO <sub>2</sub>	ZrCl <sub>4</sub> , O <sub>2</sub>	O <sub>2</sub> + Ar	ZrO <sub>2</sub> (monoclinic + tetragonal)	18–32	[Cl]
18	ZrO <sub>2</sub> - Al <sub>2</sub> O <sub>3</sub>	ZrCl <sub>4</sub> , Al, O <sub>2</sub>	O <sub>2</sub> + Ar	ZrO <sub>2</sub> (tetragonal)	17	[Cl]
19	Y <sub>2</sub> O <sub>3</sub>	Y(COOH) <sub>3</sub> , O <sub>2</sub>	O <sub>2</sub> + Ar	Y <sub>2</sub> O <sub>3</sub> (cubic)	15–25	

**Table 1.** Nanoparticles syntheses.

## 5. Particle size distribution and morphology

Granulometric composition is one of the most important nanopowders characteristics, which determines the possibility of their use in solving scientific problems and in practical applications. According to the results of electron microscopy, all nanopowders synthesized in plasma reactor are polydisperse and consist of particles of equiaxial shape (**Figure 4**). The presence of nanoobjects with oriented growth forms is not detected. Formation of nanoparticles under the conditions of plasmachemical synthesis occurs through the macro-mechanisms “vapor-liquid-crystal” (VLC), “vapor-crystal” (VC) and mixed mechanism, including a combination of these mechanisms (VLC-VC). Thermodynamic calculations of the nanopowder equilibrium yield as a function of temperature elucidate the mechanism of nanoparticle formation in a particular process.

Suppose that the substance in question exists in the liquid and solid state, and its yield depends on the temperature. Let us determine  $T^*$  as the temperature corresponding to the maximum yield of the nanoparticle substance,  $T_c$  as the maximum temperature at which the nanoparticle exists in the condensed state, and  $T_m$  as the melting temperature of nanoparticle

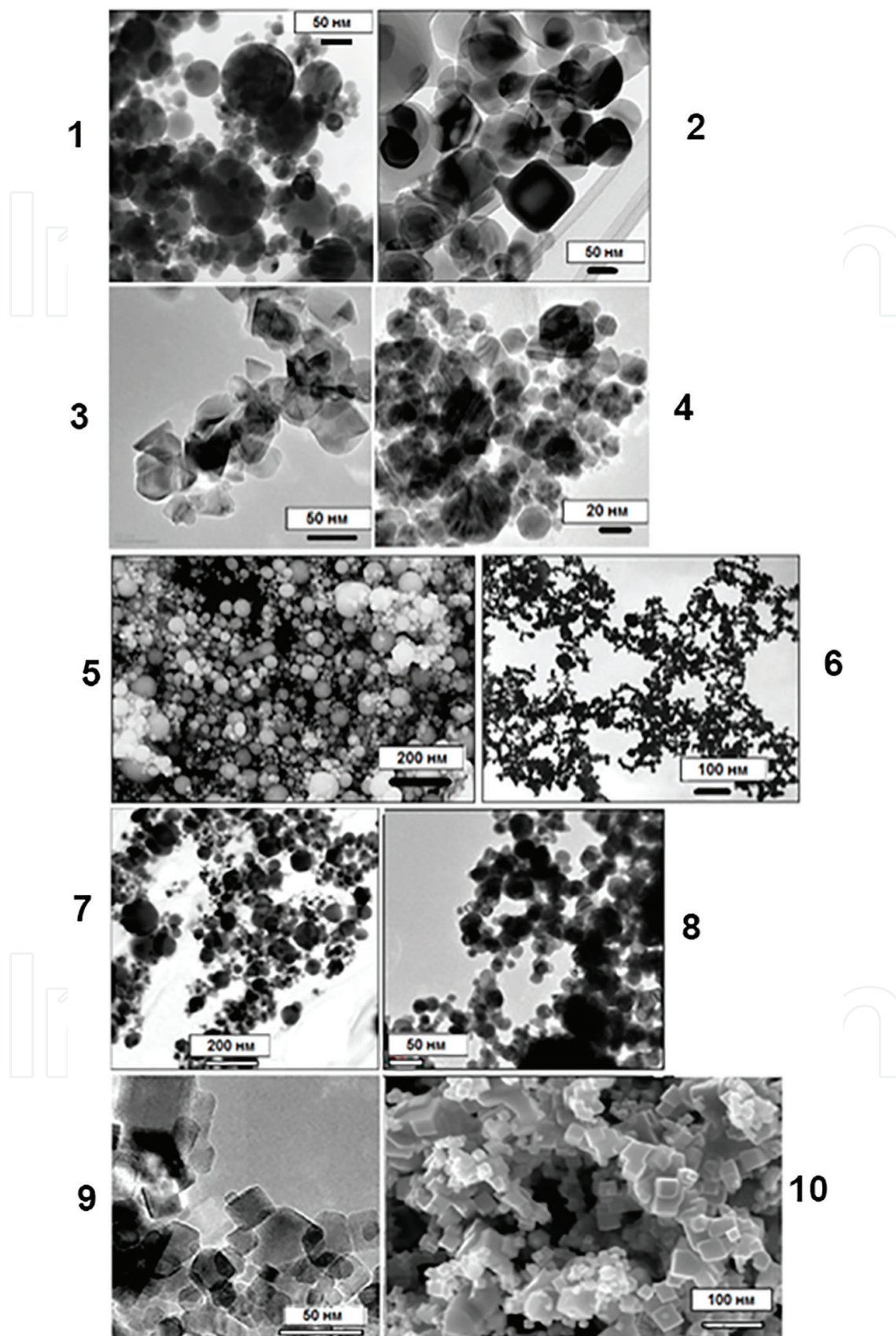


**Figure 4.** TEM and SEM micrographs. 1— $\text{Al}_2\text{O}_3$ , 2— $\text{TiO}_2$ , 3— $\text{SiC}$ , 4— $\text{W-C}$ , 5— $\text{Cu}$ , 6— $\text{W}$ , 7— $\text{W-cu}$ , 8— $\text{W-Ni-Fe}$ , 9— $\text{TiC}$ , 10— $\text{TiCN}$ .

matter. Taking into account the fact that the plasma process occurs at a decreasing temperature initially exceeding  $T_c$ , the temperature conditions for the nanoparticles formation by the above-mentioned macro-mechanisms can be written as:

mechanism VLC,  $T_m < T^* < T_c$ , all particles have a spherical habit (**Figure 5a**; 4-1; 4-5);

mechanism VC,  $T^* < T_c < T_m$ , all particles have a faceted habit (**Figure 5b**, 4-2);

mechanism of VLC-VC,  $T^* < T_m < T_c$ , particles have both spherical and faceted habit (**Figure 6c**; 4-9; 4-10).

The VLC mechanism is realized if, under conditions of a decreasing process temperature, the maximum yield of nanoparticle matter occurs at temperatures above the melting point temperature (**Figure 5a**). The VC mechanism will determine formation of nanoparticles if the formation occurs at the temperatures below the melting temperature of the nanoparticle matter (**Figure 5b**), or the substance does not exist at all in the liquid state.

If during nanoparticles formation temperature is reduced and the substance undergoes crystallization (solidification) before the maximum yield is reached, then nanoparticles formation mechanism changes from VLC to VC, and product will contain both spherical and faceted particles (**Figure 5c**). As follows from the microphotographs of the obtained nanopowders (**Figure 4**), nanoparticles formation in the realized plasma syntheses can occur through all three of these mechanisms (VLC, VC, and VLC-VC). Under plasma synthesis conditions, all of the above mechanisms took place in the formation of  $Al_2O_3$ ,  $TiO_2$ , Cu, W, TiN, TiCN and W-C composition nanoparticles. The micrographs of the nanopowders were used to construct the histograms of the particle size distribution, and statistical analysis was carried out (**Figure 6**) [19].

It was established that the lognormal particle size distribution function (PSDF) reliably (with a correlation coefficient of more than 0.95) describes all the objects under investigation over wide range of changes in the granulometric composition of the investigated nanopowders.

In the PSDF formula  $d$  is the diameter of the particle,  $m$  is the median of the distribution, and  $\sigma$  is the standard deviation. It should be emphasized, that the validity of lognormal particle size distribution was confirmed earlier for the case of nanopowders obtained in the processes where the formation of particles occurs via coagulation mechanism, i.e. VLC [20]. The experimentally established lognormal particle size distribution in the absence of coagulation growth in accordance

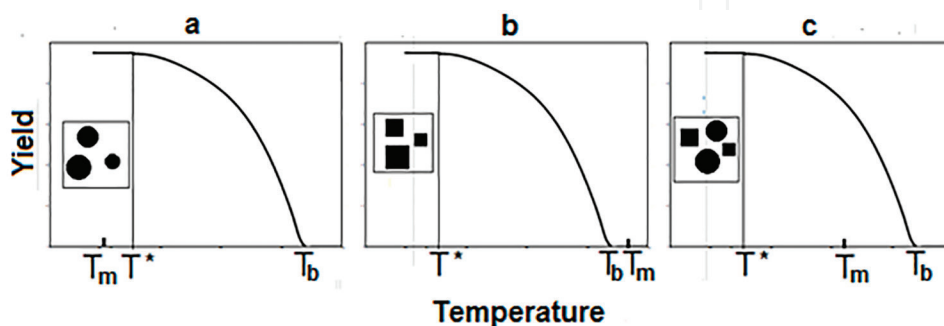


**Figure 5.** Possible characteristic relations between temperatures, when nanoparticles are formed via different mechanisms.

with [21] can be due to the lognormal distribution of the particles residence time in the growth zone. For the nanoparticles syntheses (Table 1) where formation of particles occurs through various macro mechanisms, it has been experimentally established that the average size of the nanoparticles increases with increasing concentration of the gas component precursor [22–30].

The effect of the plasma process parameters, as well as effect of the characteristic dimensions of the reactor, was studied in Ref. [24] in case of tungsten and nickel nanopowders synthesis by reduction of  $WO_3$  and NiO oxides in hydrogen-nitrogen and propane-air plasmas. It is shown that the average metal nanoparticle size can be affected by the characteristic dimensions of the

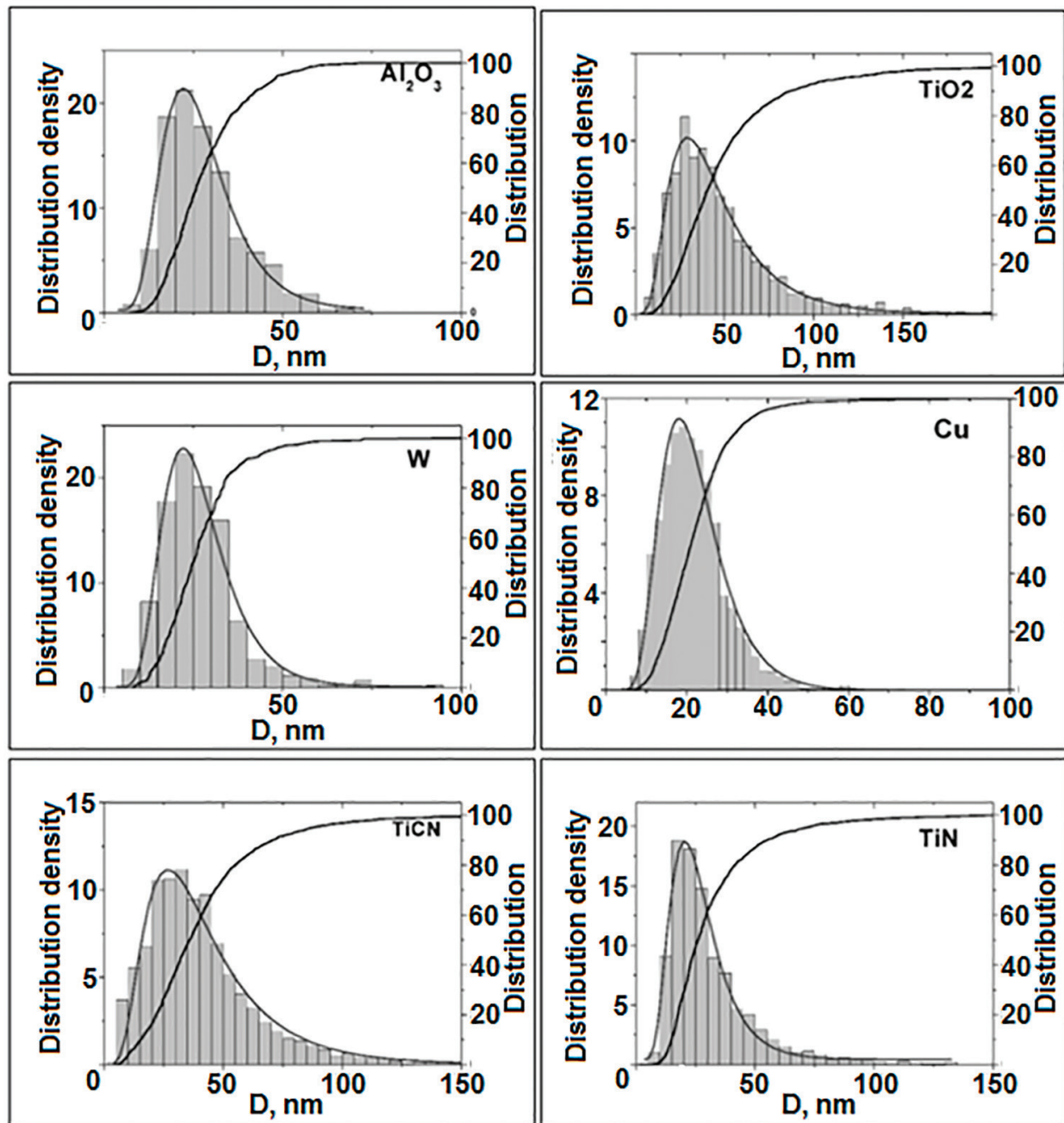


Figure 6. Particles size distributions for  $Al_2O_3$ ,  $TiO_2$ ,  $W$ ,  $cu$ ,  $TiCN$  and  $TiN$  nanopowders.

plasma apparatus, such as reactor diameter and plasma torch nozzle diameter. These parameters determine the dimensions of the high-temperature zone where the nanoparticles formation takes place. The chemical processes, occurring at nanoparticle surface, also could influence the regularities of nanoparticle growth. The results of studies of various nanopowders production in the plasma reactor indicate that the influence of the process parameters on the average particle size is a multifactor problem, where the physicochemical features of the process play significant role.

It was found that the average nanoparticle size depends on the synthesis parameters such as the initial precursor concentration, plasma jet enthalpy and velocity. The individual features of the specific process determine the degree of influence of these parameters. Production of nanoparticles of extremely small size in the confined jet reactor can be achieved only if the initial vapor concentration is significantly reduced or the jet velocity is increased. Reducing the initial concentration results in a decrease in the synthesis productivity, and the velocity increase has certain physical and technical limitations. Controlled change of nanoparticles coagulation growth time in the thermal plasma flow manipulates the size of nanoparticles, formed by the VLC mechanism. Additional channel to control the nanoparticle growth time is fast quenching by cold gas injection. Cold gas injection forces cessation of the coagulation growth after completion of vapor–liquid phase transition.

Distributed radial injection of quenching gas was organized at the periphery of the high-temperature flow in the synthesis of alumina nanopowder by oxidation of a metal powder in air plasma flow [25]. Quenching was carried out at the different distances from the reactor inlet, thus varying the particles residence time in the coagulation growth zone. The change of the injection gas flow rate and the injection position allowed the variation of the average particle size in the range of 35 to 75 nm. The obtained results indicate that confined DC plasma jet reactor is capable to produce wide range of individual elements nanopowders as well as nanopowders of inorganic compounds and composites.

## 6. Spheroidization of metal powders

Spherical powders with a particle size of the order of 10  $\mu\text{m}$  are used as starting materials for the manufacture of products from metals and alloys by the additive technologies methods. Processing of powders with irregular particle shape in thermal plasma flows ensures their fusion, leading to the formation of spherical particles [31].

Titanium powders (fractions of 40–70  $\mu\text{m}$  and less than 40  $\mu\text{m}$ ) were processed in the flow of thermal argon plasma, generated by an electric arc plasma torch. The hydrogenation-dehydrogenation process produced raw titanium powders. After plasma processing, the degree of spheroidization has reached 96%. Average sphericity coefficient was equal to 1.01 (**Figure 7**).

Experimental studies of the production of nonporous spherical powders of multicomponent metal alloys have been performed. Ultrafine powder compositions of alloy components, having a particle size of less than 1  $\mu\text{m}$ , have been used as raw material. Model high-alloy Fe-Ni-Cr alloy particles were used as example, and spherical alloy powders with particle sizes in the range from 25 to 50  $\mu\text{m}$  were produced.

The process consisted of the following stages: microgranulation of ultrafine powder, heat treatment of microgranules (drying at 100°C, removal of organic binder at 300°C, thermochemical treatment in H<sub>2</sub> at 1000°C, vacuum treatment at 1200°C), classification of heat-treated microgranules with separation of microgranules fraction in the range 25 to 50 μm, spheroidization of the isolated fraction of microgranules in the thermal plasma flow, separation of

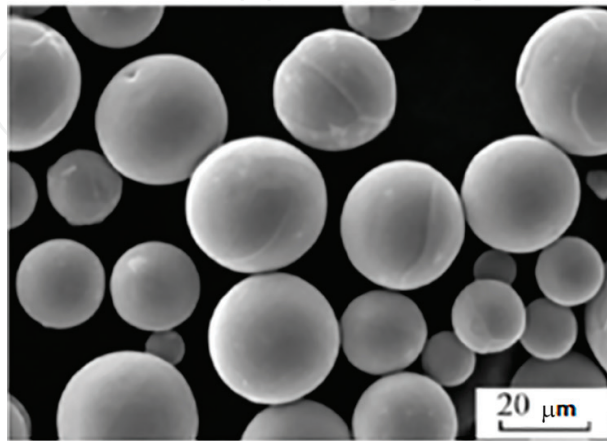


Figure 7. Micrographs of spheroidized titan powder.

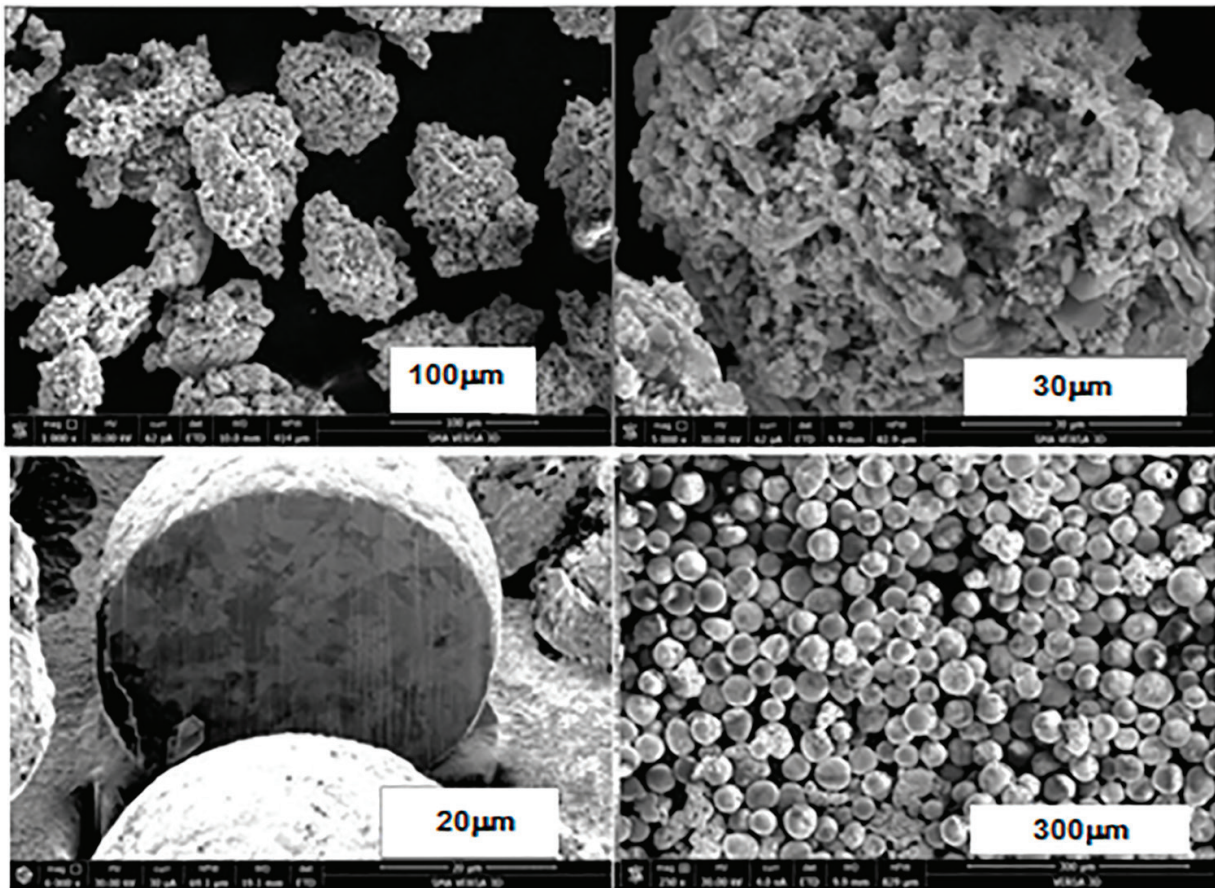


Figure 8. Micrographs of granules. (A) – Initial alloy components, (B) – Spheroidized in plasma.

the micron and submicron fraction. Micrographs of the alloy components microgranules and particles, spheroidized in the plasma flow, are shown in **Figure 8**. The presented experimental results indicate the possibility of metallic and alloys powders spheroidization in a confined DC plasma jet apparatus using various initial powder materials.

## 7. Conclusion

The presented results of research and development testify to the wide possibilities of plasma processes and devices for obtaining nanopowders of metals and their various inorganic compounds with specified properties. The nanopowders, produced in the plasma reactors, were used in various R&D projects aimed at creation of new materials with special and improved properties. Along with the production of nanopowders, the same plasma reactor with confined jet provides the possibility of metal and alloys powders spheroidizing for their application in additive technologies. The accumulated experience is the basis for the creation of efficient industrial production of powders using plasma reactors based on DC arc plasma torch.

## Acknowledgements

This work was supported by the Fund of Applied Researches, Ministry of Education and Science of the Russian Federation (unique identifier of the project RFMEFI57816X0216).

## Author details

Andrey Samokhin<sup>1</sup>, Nikolay Alekseev<sup>1</sup>, Mikhail Sinayskiy<sup>1</sup>, Aleksey Astashov<sup>1</sup>, Dmitrii Kirpichev<sup>1</sup>, Andrey Fadeev<sup>1</sup>, Yurii Tsvetkov<sup>1</sup> and Andrei Kolesnikov<sup>2\*</sup>

\*Address all correspondence to: avkolesnikov@yahoo.com

1 A. Baikov Institute of Metallurgy and Materials Science (IMET RAS), Moscow, Russia

2 Tshwane University of Technology (TUT), Pretoria, South Africa

## References

- [1] Gogotsi Y, editor. *Nanomaterials Handbook*. 2nd ed. Boca Raton: CRC Press; 2006. p. 682
- [2] Koch CC, editor. *Nanostructured Materials: Processing, Properties and Applications*. 2nd ed. Norwich: William Andrew; 2006. p. 784
- [3] Wang ZL, Liu Y, Zhang Z, editors. *Handbook of nanophase and nanostructured materials*. vol. IV, Berlin: Springer; 2002. p. 1200
- [4] Shaw D, Liu B, editors. *Handbook of Micro and Nanoparticle Science and Technology*. Berlin: Springer Verlag; 2007. p. 2400

- [5] Hosokawa M, Nogi K, Naito M, Yokoyama T, editors. Nanoparticle Technology Handbook. 2nd ed. Amsterdam: Elsevier; 2008. p. 730
- [6] Liu LJ, Bashir S. Advanced Nanomaterials and Their Applications in Renewable Energy. Amsterdam: Elsevier Science; 2015. p. 436
- [7] Gromov AA, Korotkikh A G, Il'in A, DeLuca LT, Arkhipov VA, Monogarov KA, Teipel U. Nanometals: Synthesis and Application in Energetic Systems. In: Energetic nanomaterials: Synthesis, characterization, and application. Amsterdam: Elsevier Science; 2016. p. 47-63. DOI: 10.1016/B978-0-12-802710-3.00003-9
- [8] Altavilla C, Ciliberto E, editors. Inorganic Nanoparticles: Synthesis, Applications, and Perspectives. Boca Raton: CRC Press; 2010. p. 576
- [9] Andrievski RA. Nanomaterials based on high-melting carbides, nitrides and borides. Russian Chemical Reviews. 2005;74:1061-1072 <https://doi.org/10.1070/RC2005v074n12ABEH001202>
- [10] Toumanov YN. Plasma, High-Frequency, Microwave and Laser Technologies in Chemical and Metallurgical Processes (in Russian). Moscow: Fizmatlit; 2010. p. 968
- [11] TEKNANO Nanopowder Synthesis Systems. 2016. Available from <http://www.tekna.com/nanopowder-synthesis-systems>
- [12] Roth JR. Industrial Plasma Engineering, Volume 1: Principles. Boca Raton: CRC Press; 1995. p. 339
- [13] Zhukov MF, Zasytkin IM, Timoshevskii AN, Mikhailov BI, Desyatkov GA. Electric Arc Generators of Thermal Plasma (in Russian). Nauka: Novosibirsk; 1999. p. 712
- [14] Plasma Torches by Westinghouse Plasma Corporation. 2005. Available from [https://www.academia.edu/24044626/Plasma\\_Torches\\_by\\_Westinghouse\\_Plasma\\_Corporation](https://www.academia.edu/24044626/Plasma_Torches_by_Westinghouse_Plasma_Corporation)
- [15] Mikhailov BI. Electric-arc plasmachemical reactors of separated, single-chamber, and combined types. Thermophysics and Aeromechanics (Teplofizika i aeromekhanika). 2010;17(3):425-440
- [16] Samokhin AV, Astashov AG, Alekseev NV, Tsvetkov YV. Characteristics of heat and mass transfer to the wall of a confined-jet plasma flow reactor in the processes of nanopowder preparation from metals and their compounds. Nanotechnologies in Russia. 2016;11(1-2): 57-62. DOI: 10.1134/S1995078016010134
- [17] Alekseev NV, Samokhin AV, Tsvetkov YuV. Plasma plant for manufacturing of nanodispersed powders (in Russian). RF Patent No 2311225. 2007
- [18] Mädler L, Friedlander SK. Transport of nanoparticles in gases: Overview and recent advances. Aerosol and Air Quality Research. 2007;7(3):304-342. DOI: 10.4209/aaqr.2007.03.0017
- [19] Sinayskiy MA, Samokhin AV, Alekseev NV, Tsvetkov YV. Extended characteristics of dispersed composition for nanopowders of plasmachemical synthesis. Russian Nanotechnologies. 2016;11(11-12):110-115. DOI: 10.1134/S1995078016060185

- [20] Granqvist CG, Buhrman RA. Ultrafine metal particles. *Journal of Applied Physics*. 1976;**47**:2200-2219. DOI: 10.1063/1.322870
- [21] Kiss LB, Soderlund J, Niklasson GA, Granqvist CG. New approach to the origin of lognormal size distributions of nanoparticles. *Nanotechnology*. 1999;**10**:25-28. DOI: 10.1088/0957-4484/10/1/006
- [22] Alekseev NV, Balikhin IL, Kurkin EN, et al. Formation of ultrafine aluminum oxide powder in confined air plasma jet (in Russian). *Fizika I Khimiya Obrabotki Materialov (Physics and Chemistry of Materials Processing)*. 1994;**4-5**:72-78
- [23] Alekseev NV, Balikhin IL, Kurkin EN, Samokhin AV, Troitskaya EV, Troitskii VN. Synthesis of titanium nitride and carbonitride ultradisperse powders in nitrogen plasma jet (in Russian). *Fizika I Khimiya Obrabotki Materialov (Physics and Chemistry of Materials Processing)*. 1995;**1**:31-39
- [24] Alekseev NV, Samokhin AV, Grechikov MI. Controlling the granulometric composition of the metal powders produced in plasma reduction processes (in Russian). *Fizika I Khimiya Obrabotki Materialov (Physics and Chemistry of Materials Processing)*. 1997;**6**:54-60
- [25] Alekseev NV, Samokhin AV, Kurkin EN, Агафонов KH, Tsvetkov YV. Synthesis of alumina nanoparticles by metal oxidation in thermal plasma flows (in Russian). *Fizika I Khimiya Obrabotki Materialov (Physics and Chemistry of Materials Processing)*. 1997;**3**:33-39
- [26] Alekseev NV, Samokhin AV, Tsvetkov YV. Synthesis of titanium carbonitride nanopowder by titanium tetrachloride processing in hydrocarbon-air plasma. *High Energy Chemistry*. 1999;**33**(3):194-197
- [27] Kolesnikov A, Alexeev N, Samokhin A. Controlled synthesis of alumina nanoparticles in a reactor with self-impinging plasma jets. *International Journal of Chemical Reactor Engineering*. 2007;**5**:A95. DOI: 10.2202/1542-6580.1521
- [28] Samokhin AV, Polyakov SN, Astashov AG, Alekseev NV, YuV T. Simulation of nanopowders synthesis in a jet type reactor. II. Formation of nanoparticles (in Russian). *Fizika I Khimiya Obrabotki Materialov (Physics and Chemistry of Materials Processing)*. 2014;**3**:12-17
- [29] Samokhin AV, Sinayskiy MA, Alekseev NV, et al. Synthesis of nanoscale zirconium dioxide powders and composites on their basis in thermal DC plasma. *Inorganic Materials: Applied Research*. 2015;**6**:528-535. DOI: 10.1134/S2075113315050172
- [30] Kotlyarov VI, Beshkarev VT, Kartsev VE, et al. Production of spherical powders on the basis of group IV metals for additive manufacturing. *Inorganic Materials: Applied Research*. 2017;**8**(3):452-458. DOI: 10.1134/S2075113317030157
- [31] Samokhin AV, Fadeev AA, Sinayskiy MA, et al. Fabrication of high-alloy powders consisting of spherical particles from ultradispersed components. *Russian Metallurgy (Metally)*. 2017;**7**:547-553. DOI: 10.1134/S0036029517070138